MULTI-SCALE EXPOSURE FUSION VIA GRADIENT DOMAIN GUIDED IMAGE FILTERING

Fei Kou[1,2], Zhengguo Li[3], Changyun Wen[4], and Weihai Chen[1,*]

[1] School of Automation Science and Electrical Engineering, Beihang University, Beijing, China
[2]New Technical Institute, vivo Mobile Communication Co. Ltd., Hangzhou, China
[3]Robotics Department, Institute for Infocomm Research, 1 Fusionopolis Way, Singapore
[4]School of Electrical and Electronic Engineering, Nanyang Technological University, Singapore

ABSTRACT

Multi-scale exposure fusion is an efficient way to fuse differently exposed low dynamic range (LDR) images of a high dynamic range (HDR) scene into a high quality LDR image directly. It can produce images with higher quality than single-scale exposure fusion, but has a risk of producing halo artifacts and cannot preserve details in brightest or darkest regions well in the fused image. In this paper, an edge-preserving smoothing pyramid is introduced for the multi-scale exposure fusion. Benefiting from the edge-preserving property of the filter used in the algorithm, the details in the brightest/darkest regions are preserved well and no halo artifacts are produced in the fused image. The experimental results prove that the proposed algorithm produces better fused images than the state-of-the-art algorithms both qualitatively and quantitatively.

Index Terms— Exposure fusion, image pyramid, gradient domain guided image filter, edge-preserving smoothing, high dynamic range

1. INTRODUCTION

Most natural scenes have larger dynamic ranges than the dynamic range that can be recorded by a regular camera with a single shot. As a result, an image captured by the camera is not the same as what human eyes see. This challenge can be addressed by taking several differently exposed low dynamic range (LDR) images for the same scene and merging them together [1, 2]. The technique can be used to achieve that what we captured is what our human eyes see. Such an imaging technique is called HDR imaging [3, 4]. Due to possible camera movement and moving objects, all the LDR images are first aligned [5] and all the moving objects are synchronized according to a pre-defined reference image [6, 7]. The synchronized multiple exposure images are then adopted to synthesize a high dynamic range (HDR) image [2]. The HDR image is finally tone mapped as an LDR image so as to be displayed on a conventional LDR display [8, 9, 10, 11].

There is an alternative approach called exposure fusion which fuses an exposure bracket into a high quality LDR image directly. Mertens et al. [12] used a Laplacian pyramid [13] to decompose all the differently exposed images and a Gaussian pyramid [13] to smooth the weighted maps that are computed considering the contrast, saturation and well-exposedness. Shen et al. [14] proposed a generalized random walks framework based exposure fusion algorithm to achieve an optimal balance between local contrast and color consistency while combining the scene details revealed under different exposures. Ma et al. [15] introduced a patch-wise exposure fusion approach. In this approach, the patches in the input images are decomposed into three components: signal strength, signal structure and mean intensity. The three components are processed separately and finally a fused image is constructed. Exposure fusion neither requires lighting conditions of all the LDR images to be the same nor requires knowledge of exposure times as required by the HDR imaging [1, 2]. However, there is no fine detail extraction component in the exposure fusion algorithms while fine details can be manipulated by existing tone mapping algorithms [10, 11]. Based on such an observation, a detail extraction component was proposed in [16] to enhance the existing exposure fusion algorithms. Recently, an interesting subjective user study was conducted in [17] to evaluate the quality of images generated by the above exposure fusion algorithms. It was found that no single state-of-the-art exposure fusion algorithm produces the best quality for all test images. The algorithm in [12] achieves the best performance on average, and the algorithm in [16] is the second best on average.

Even though the global contrast is preserved better by the existing multi-scale exposure fusion algorithms, fine details in brightest/darkest regions could be lost if there are too many scales. It is thus necessary to properly select the number of scales to preserve both the global contrast and fine de-

This work has been supported by National Nature Science Foundation of China under the research project 61620106012, 61573048 and by the International Scientific and Technological Cooperation Projects of China under Grant No.2015DFG12650.

*(Corresponding author: Weihai Chen.)

tails in the brightest/darkest regions. Unfortunately, this is impossible using the existing Gaussian pyramid in [13] due to possible halo artifacts. It is desired to develop a new pyramid for exposure fusion. Existing edge-preserving smoothing techniques [10, 18, 19, 20, 21, 22] are good at reducing or avoiding halo artifacts from appearing in images that are produced using them. Intuitively, edge-preserving smoothing techniques might be applied to design an exposure fusion algorithm to fuse differently exposed images without halo artifacts. However, it was indicated in [12] that it is very difficult or even impossible to use the edge-preserving smoothing techniques such as the bilateral filter in [18] to design an exposure fusion algorithm without producing halo artifacts. In addition, the exposure fusion algorithm in [23] which is based on the guided image filter (GIF) in [19] indeed produces visible halo artifacts in fused images. It seems that the possibility of using edge-preserving smoothing techniques to design an exposure fusion algorithm without producing halo artifacts is very low. Fortunately, the exposure fusion algorithm in [23] is only a two-scale one and it was shown in [12] that halo artifacts could be reduced/avoided if the number of scales is increased. Thus, there is still a chance to design a new edge-preserving smoothing pyramid to replace the existing Gaussian smoothing pyramid for the multi-scale exposure fusion.

In this paper, an elegant edge-preserving smoothing pyramid is proposed for the multi-scale exposure fusion. All the differently exposed images are decomposed using the Laplacian pyramid as in [12]. A weighting map is computed for each image by considering the contrast, saturation and well-exposedness of each pixel as in [12]. Instead of using the Gaussian pyramid to smooth the weighting maps as in [12], an edge-preserving smoothing pyramid is introduced to smooth the weight maps. Particularly, the new edge-preserving smoothing pyramid is designed using the gradient domain GIF (GGIF) in [22] with the guided images being selected as the luminance components of the differently exposed images. The structure of the luminance component of each input image is transferred to the corresponding weight map by the GGIF. With the GGIF based pyramid, the details in the brightest and darkest regions are preserved much better than [12]. Experimental results show that the proposed algorithm indeed produces better fused images than the state-of-the-art algorithms from both subjective and objective points of view. Overall this paper has the following three major contributions: 1) an edge-preserving smoothing pyramid; 2) a state-of-the-art multi-scale exposure fusion algorithm; and 3) a novel application of edge-preserving smoothing techniques.

The remainder of this paper is organized as follows. Details on smoothing of weight maps via the GGIF is provided in the next section. The edge-preserving smoothing pyramid based exposure fusion is proposed in the section 3, followed by the experimental results of the proposed algorithm with comparison to several other state-of-the-art algorithms in Section 4. Finally Section 5 concludes this paper.

2. SMOOTHING OF WEIGHT MAPS VIA THE GGIF

2.1. Construction of weight maps

Given a set of differently exposed images I_k with the subscript k indexing the image number. The image set contains flat, colorless regions due to under- and over-exposure. All these regions should give less weight, while well-exposed regions containing bright colors and details should give more weight. There are many interesting ways to define the weight maps. To illustrate advantage of the edge-preserving smoothing pyramid with respect to the Gaussian pyramid, the weight maps in [12] is adopted in this paper.

Let p be a pixel position. There are three quality measures in [12], $C_k(p)$, $S_k(p)$, and $E_k(p)$ measure contrast, color saturation, and well-exposedness of pixel $Z_k(p)$, respectively. $C_k(p)$ is obtained by applying a Laplacian filter to the gray-scale version of each image. $S_k(p)$ is computed as the standard deviation within the R, G and B channel. $E_k(p)$ is yielded by multiplying the well-exposedness of each color channel obtained by applying a Gaussian curve to each channel separately. The product of the three quality measure is denoted as $\tilde{W}_k(p)$. The weight map is then constructed as $W_k(p) = \tilde{W}_k(p) / \sum_{k'=1}^{N} \tilde{W}_{k'}(p)$.

2.2. Edge-preserving smoothing of weight maps

The weight map $W_k(p)$ was smoothed using the Gaussian filter in [12]. In the proposed algorithm, it is smoothed using the GGIF [22] with the guidance image as the luminance component of the image I_k. Compared with the Gaussian filter in [12], the GGIF has two advantages. One is that edges are preserved better by the GGIF. Thus halo artifacts can be avoided even though the number of layers is reduced in the proposed exposure fusion algorithm. The other is that the structure of the luminance component of each input image is transferred to the corresponding weight map. As a result, fine details in the brightest/darkest region are preserved much better using the proposed algorithm.

The weighted map $W_k(p)$ is decomposed into two parts as follows:

$$W_k(p) = W_{k,b}(p) + W_{k,d}(p), \tag{1}$$

where $W_{k,b}(p)$ is a base layer formed by homogeneous regions with sharp edges, $W_{k,d}(p)$ is a detail layer formed by fine details.

Let $\Omega_\zeta(p)$ be a square window centered at the pixel p of a radius ζ. It is assumed that $W_{k,b}(p)$ is a linear transform of the luminance component Y_k in the window $\Omega_\zeta(p')$:

$$W_{k,b}(p) = a_{k,p'} Y_k(p) + b_{k,p'}, \forall p \in \Omega_\zeta(p'), \tag{2}$$

where $a_{k,p'}$ and $b_{k,p'}$ are two constants in the window $\Omega_\zeta(p')$.

The values of $a_{k,p'}$ and $b_{k,p'}$ are obtained by minimizing the following cost function $E(a_{k,p'}, b_{k,p'})$:

$$\sum_{p\in\Omega_\zeta(p')} [(a_{k,p'}Y_k(p) + b_{k,p'} - W_k(p))^2 + \lambda \cdot (a_{k,p'} - \gamma_{p'})^2/\Gamma_{Y_k}(p')], \quad (3)$$

where λ is a regularization parameter penalizing large $a_{k,p'}$. $\Gamma_{Y_k}(p')$ is and $\gamma_{p'}$ are two edge aware weighting based on normalized two-scale neighbourhood variance $\sigma(p')$, defined as follows:

$$\Gamma_{Y_k}(p') = \frac{1}{M}\sum_{p=1}^{N}\frac{\sigma^2_{Y_k}(p')+\varepsilon}{\sigma^2_{Y_k}(p)+\varepsilon}, \quad (4)$$

$$\gamma_{p'} = \frac{1}{1+e^{\eta(\sigma^2_{Y_k}(p') - \mu_{\bar{\sigma^2_{Y_k}}})}}, \quad (5)$$

where M is the total number of pixels in an image. ε is a small constant and its value is selected as $(0.001 \times L)^2$ while L is the dynamic range of the input image, $\mu_{\bar{\sigma^2_{Y_k}}}$ is the mean value of all $\sigma^2_{Y_k}(p)$, η is calculated as $4/(\mu_{\bar{\sigma^2_{Y_k}}} - \min(\sigma^2_{Y_k}(p)))$.

3. FUSION OF DIFFERENTLY EXPOSED IMAGES

3.1. Laplician pyramids of differently exposed images

Given the set of differently exposed images I_k. The Gaussian pyramids of the k-th weight map W_k and the Laplacian pyramids of the k-th input image I_k are produced for all k using the method in [13]. Let the l-th layer of the Gaussian pyramid and the Laplacian pyramid be defined as $\mathbf{G}\{I\}_k^{(l)}$ and $\mathbf{L}\{I\}_k^{(l)}$. In $\mathbf{G}\{I\}_k^{(l)}$, the first layer $\mathbf{G}\{I\}_k^{(0)}$ is the input image, the $l(\geq 1)$ layer $\mathbf{G}\{I\}_k^{(l)}$ is a down-sampled Gaussian smoothed version of the $(l-1)$th layer $\mathbf{G}\{I\}_k^{(l-1)}$. In the Laplacian pyramid, the l-th layer $\mathbf{L}\{I\}_k^{(l)}$ is generated by deducting the up-sampled version of $\mathbf{G}\{I\}_k^{(l+1)}$ from $\mathbf{G}\{I\}_k^{(l)}$.

Define a constant κ as $\lfloor \log_2 \min(r,c) \rfloor$, where $\lfloor x \rfloor$ returns the largest integer which is smaller than or equal to x. r and c are the number of pixel rows and columns of the input image. We shall now evaluate the influence of the pyramid layer to the Gaussian pyramid and the proposed edge-preserving smoothing pyramid by testing two image sets "treeunil" and "tower". In the proposed edge-preserving smoothing pyramid, the radius ζ is selected as 1, 2, 4, 8 for κ, $(\kappa-1)$, $(\kappa-2)$, $(\kappa-3)$ respectively, and λ is set to $1/1024$. The objective metric in [17] is used to evaluate the quality of the fused images, with results summarized in Table 1. From the table, it can be found that when the number of layers is selected as $(\kappa-2)$, fused images have the highest scores. Also from the table, it can be concluded that with layer less than $(\kappa-1)$, the objective quality of the fused image with the Gaussian pyramid could be dropped. As shown in Fig. 1, there are halo artifacts (the color of the sky becomes brighter near the trees and mountains) if the number of layers is less than κ. Thus, the number of layers is selected as κ in [12] while it is selected as $(\kappa-2)$ in the proposed algorithm.

Table 1. MEF-SSIM of two different pyramids.

	κ	$\kappa-1$	$\kappa-2$	$\kappa-3$
Gaussian	0.9858	0.9870	**0.9876**	0.9818
GGIF	0.9859	0.9883	**0.9904**	0.9878
Gaussian	0.9499	**0.9583**	0.9525	0.9365
GGIF	0.9497	0.9603	**0.9628**	0.9555

(a) κ (b) $(\kappa-1)$ (c) $(\kappa-2)$

(d) Zoom in of (a) (e) Zoom in of (b) (f) Zoom in of (c)

Fig. 1. Comparison of different layers with image set "treeunil" for the Gaussian pyramid.

3.2. GGIF pyramids of weight maps

The weight maps of all the different exposed images I_k are first calculated using equation (**??**), and they are then used to produce the corresponding Gaussian pyramids $\mathbf{G}\{W\}_k^{(l)}$. The GGIF pyramids of the weight maps are finally obtained as follows:

Through solving the optimization problem in equation (3), the optimal values of $a_{k,p'}^{(l)}$ and $b_{k,p'}^{(l)}$ are obtained. The final value of $W_{k,b}^{(l)}(p)$ is then given as follows:

$$W_{k,b}^{(l)}(p) = \bar{a}_{k,p}^{(l)} Y_k^{(l)}(p) + \bar{b}_{k,p}^{(l)}, \quad (6)$$

where $\bar{a}_{k,p}^{(l)}$ and $\bar{b}_{k,p}^{(l)}$ are the mean values of computed as $a_{k,p'}^{(l)}$ and $b_{k,p'}^{(l)}$ in the window $\Omega_\zeta(p')$, respectively.

3.3. Fusion of differently exposed images

Once the Laplacian pyramids of the k-th input image $\mathbf{L}\{I\}_k^{(l)}$ and the edge-preserving pyramid of the weighing maps $\mathbf{E}\{W\}_k^{(l)}$ are constructed, a Laplacian pyramid of the resultant fused image R can be obtained via:

$$\mathbf{L}\{R\}^{(l)}(p) = \sum_{k=1}^{N} \mathbf{E}\{W\}_k^{(l)}(p)\mathbf{L}\{I\}_k^{(l)}(p), \quad (7)$$

(a) Result by [14] (b) Result by [16] (c) Result by [23] (d) Result by [15] (e) Result by [12] (f) Result by ours

(g) Zoom in of (a) (h) Zoom in of (b) (i) Zoom in of (c) (j) Zoom in of (d) (k) Zoom in of (e) (l) Zoom in of (f)

Fig. 2. Comparison of different exposure fusion algorithms with image set "treeunil".

(a) Result by [14] (b) Result by [16] (c) Result by [23] (d) Result by [15] (e) Result by [12] (f) Result by ours

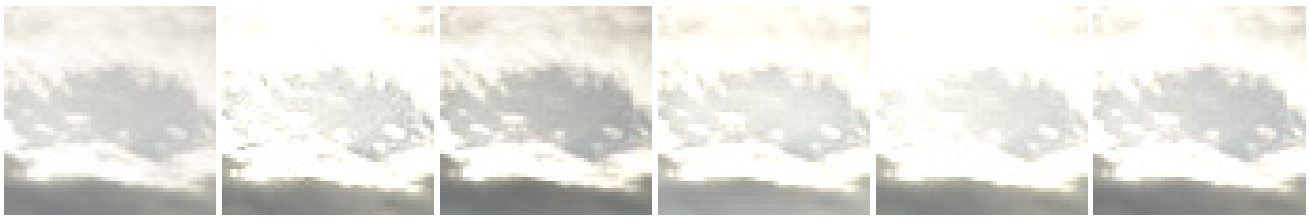

(g) Zoom in of (a) (h) Zoom in of (b) (i) Zoom in of (c) (j) Zoom in of (d) (k) Zoom in of (e) (l) Zoom in of (f)

Fig. 3. Comparison of different exposure fusion algorithms with image set "tower".

and the final resultant image can be obtained by reconstructing the Laplacian pyramid $\mathbf{L}\{R\}$.

4. EXPERIMENTAL RESULTS

In this section, the proposed exposure fusion algorithm is compared with five state-of-the-art exposure fusion algorithms respectively given in [12], [16], [23], [14], [15]. Among these five algorithms, the one in [12] is the best exposure fusion algorithm, according to the subjective quality assessment for multi-exposure image fusion in [17]. The algorithm in [16] is the second best and it includes a unique detail enhancement component. The algorithm in [23] is a two-scale exposure fusion algorithm and it is also based on edge-preserving smoothing technique. The algorithms in [14, 15] are two single-scale exposure fusion algorithms which attracts lots of attention.

Table 2. Comparison of six different algorithms on preserving global contrast and details in saturated regions as well as avoiding halo artifacts.

Algorithm	Global contrast	No halo	Details in saturated regions
[14]		√	√
[16]	√	√	
[23]	√		√
[15]	√		√
[12]	√	√	
Ours	√	√	√

(a) Result by [14] (b) Result by [16] (c) Result by [23] (d) Result by [15] (e) Result by [12] (f) Result by ours

(g) Result by [14] (h) Result by [16] (i) Result by [23] (j) Result by [15] (k) Result by [12] (l) Result by ours

(m) Result by [14] (n) Result by [16] (o) Result by [23] (p) Result by [15] (q) Result by [12] (r) Result by ours

Fig. 4. Comparison of different exposure fusion algorithms with image sets "BeligumHouse", "SevenEleven" and "Memorial".

Five sets of differently exposed images are tested. The experimental results are shown in Figs. 2-4. The performances of the six algorithms are summarized and listed in Table 2. From all these resultant images, it can be observed that the proposed algorithm can generate fused images with both good global contrast and good details in saturated regions. The algorithm in [14] can preserve details without producing halo, but the global contrast is not preserved well. The algorithm in [16] can enhance details of fused image, but the details in saturated region are still lost, e.g. the clouds in Fig. 2(h). The algorithm in [23] is an edge-preserving filter based algorithm. It is seen that it can preserve details in brightest/darkest regions well, but it suffers from halo artifacts, as demonstrated in Figs. 2(c), 3(c), 4(c) and 4(i). The algorithm in [15] preserves details in the brightest/darkest regions well but it also suffers from halo artifacts, as illustrated in Figs. 2(d), 4(d) and 4(j), and the global contrast is not preserved well. The algorithm in [12] is based on the Gaussian pyramid, it is seen that the global contrast is preserved well but details in brightest and darkest regions are not preserved well in several fused images. From zooming in patches in Fig. 2, it can be observed that the algorithms in [16, 15, 12] also suffers from color distortion. The objective metric in [17] is also adopted here to compare the different algorithms, with scores given in Table 3. From Table 3, it can be found that the proposed edge-preserving smoothing pyramid based exposure fusion algorithm ranks first in 4 sets of tested images and its overall average also ranks first. Thus, the proposed algorithm produces better fusion images than the state-of-the-art algorithms from both subjective and objective points of view. On the other hand, it should be mentioned that the complexity of the proposed algorithm is higher than other algorithms.

Table 3. MEF-SSIM of six different algorithms.

	Set 1	Set 2	Set 3	Set 4	Set 5	Average	Rank
[14]	0.904	0.954	0.945	0.960	0.958	0.944	6
[16]	0.925	0.956	0.952	0.944	0.954	0.946	5
[23]	0.956	0.986	0.956	0.971	**0.980**	0.970	3
[15]	0.941	0.980	0.965	0.960	0.971	0.963	4
[12]	0.950	0.986	0.974	0.969	0.976	0.971	2
Ours	**0.963**	**0.990**	**0.977**	**0.975**	0.978	**0.977**	**1**

5. CONCLUSION AND REMARKS

In this paper, an edge-preserving smoothing pyramid has been proposed for the multi-scale exposure fusion. Experimental results show that the proposed algorithm produces better fusion images than the state-of-the-art algorithms. It can be expected that the proposed pyramid is also useful in other image fusion applications, and other popular edge-preserving smoothing techniques can be applied to design a similar exposure fusion algorithm.

It is worth noting that the complexity of the proposed algorithm could be an issue for mobile devices. Fortunately,

the complexity could be reduced by using a hybrid pyramid. The gradient domain guided image filter (GGIF) is only used in a few layers with the smallest sizes while the Gaussian filter is used in all other layers. The coefficients of the GGIF is only computed at the layer with the smallest size and they are upsampled to produce the coefficients at the other layers. As such, a good trade-off between the quality and complexity can be obtained.

6. REFERENCES

[1] S. Mann and R. W. Picard, "On being 'undigital' with digital cameras: extending dynamic range by combining differently exposed pictures", in *Proc. of the 1995 IS&T's 48th Annual Conference*, pp. 442-448, 1995.

[2] P. E. Debevec and J. Malik, "Recovering high dynamic range radiance maps from photographs", in *Proc. of the 1997 Conference on Computer Graphics (SIGGRAPH)*, pp. 369-378, 1997.

[3] E. Reinhard, W. Heidrich, P. Debevec, S. Pattanaik, G. Ward, and K. Myszkowski, "High dynamic range imaging: acquisition, display, and image-based lighting", Morgan Kaufmann, 2010.

[4] R. Mantiuk, K. Myszkowski, and H.-P. Seidel, "High dynamic range imaging," in Wiley Encyclopedia of Electrical and Electronics Engineering. pp.1C42, Jun. 2015.

[5] S. Q. Wu, Z. G. Li, J. H. Zheng, and Z. J. Zhu, "Exposure robust method for aligning differently exposed images", IEEE Signal Processing Letter, vol. 21, no. 7, pp. 885-889, Jul. 2014.

[6] J. H. Zheng, Z. G. Li, Z. J. Zhu, S. Q. Wu, and S. Rahardja, "Hybrid patching for a sequence of differently exposed images with moving objects," IEEE Trans. on Image Processing, vol. 22, no. 12, pp.5190-5201, Dec. 2013.

[7] Z. G. Li, J. H. Zheng, Z. J. Zhu, and S. Q. Wu, "Selectively detail-enhanced fusion of differently exposed images with moving objects", IEEE Trans. on Image Processing, vol. 23, no. 10, pp. 4372-4382, Oct. 2014.

[8] F. durand, and J. Dorsey, "Fast bilateral filtering for the display of high-dynamic-range images", Acm Trans. on Graphics, vol. 21, no. 3 pp. 257-266, Jul. 2002.

[9] E. Reinhard, M. Stark, P. Shirley, and J. Ferwerda, "Photographic tone reproduction for digital images", ACM Trans. on Graphics, vol. 21, no. 3, pp. 267276, Jul. 2002.

[10] Z. Farbman, R. Fattal, D. Lischinski, and R. Szeliski, "Edge-preserving decompositions for multi-scale tone and detail manipulation", In *ACM SIGGRAPH 2008*, pp. 1-10, Aug. 2008, USA.

[11] Z. G. Li and J. H. Zheng, "Visual salience based tone mapping for high dynamic range images", IEEE Trans. on Industrial Electronics, vol. 61, no. 12, pp. 7076-7082, Dec. 2014.

[12] T. Mertens, J. Kautz, and F. V. Reeth, "Exposure fusion: a simple and practical alternative to high dynamic range photography", Computer Graphics Forum, Vol. 28, pp.161-171, 2009.

[13] P. Burt and E. Adelson, "The Laplacian pyramid as a compact image code", IEEE Trans. on Communications, vol. 31, pp. 532-540, 1983.

[14] R. Shen, I. Cheng, J. Shi, and A. Basu, "Generalized random walks for fusion of multi-exposure images," IEEE Trans. on Image Processing, vol. 20, pp. 3634-3646, 2011.

[15] K. D. Ma and Z. Wang, "Multi-exposure image fusion: A patch-wise approach.", in *2015 IEEE International Conference on Image Processing (ICIP)*, pp.1717-1721, 2015.

[16] Z. G. Li, J. H. Zheng, and S. Rahardja, "Detail-enhanced exposure fusion", IEEE Trans. on Image Processing, vol. 21, no 11, pp. 4672- 4676, Nov. 2012.

[17] K. D. Ma, K. Zeng, and Z. Wang, "Perceptual quality assessment for multiexposure image fusion", IEEE Trans. on Image Process., vol. 24, no. 11, pp. 3345-3356, Nov. 2015.

[18] C. Tomasi and R. Manduchi, "Bilateral filtering for gray and color images," in *1998 6th IEEE Int. Conf. on Computer Vision (ICCV1998)*, pp. 836-846, Jan. 1998. India.

[19] K. He, J. Sun, and X. Tang, "Guided image filtering," IEEE Trans. On Pattern Analysis and Machine Learning, vol. 35, no. 6, pp. 1397-1409, Jun. 2013.

[20] Z. G. Li, J. H. Zheng, Z. J. Zhu, W. Yao, and S. Q. Wu, "Weighted guided image filtering," IEEE Trans. on Image Processing. vol. 24, no.1, pp. 120-129, Jan. 2015.

[21] F. Kou, W. H. Chen, Z. G. Li, and C. Y. Wen, "Content adaptive image detail enhancement," IEEE Signal Processing Letters, vol. 22, no. 2, pp. 211-215, Feb. 2015.

[22] F. Kou, W. H. Chen, C. Y. Wen, and Z. G. Li, "Gradient domain guided image filtering," IEEE Trans. on Image Processing, Vol.24, No.11, pp. 4528 - 4539, 2015.

[23] S. T. Li, X. D. Kang, and J. Hu, "Image fusion with guided filtering", IEEE Trans. on Image Processing, vol. 22, no. 7, pp. 2864-2875, Jul. 2013.